

Rev. Letters **17**, 903 (1966); P. Kaw, E. Valio, and J. M. Dawson, *ibid.* **25**, 430 (1970); Morihiro' Josely, Electronics Laboratory Research Report No. 676, Tokyo, 1967 (unpublished).

³Lee and Su (Ref. 1).

⁴In the course of the calculations we have considered only the Landau damping and neglected the collisional damping (see DuBois and Goldman, Ref. 1). Since the Landau damping $\gamma_p \rightarrow 0$ when $k \rightarrow 0$, this must be con-

sidered a lower boundary on the permitted values of k .

⁵ γ_a will be proportional to a term containing the factor $(\omega - \mathbf{k} \cdot \mathbf{v}_D)$, v_D being the electronic drift velocity, a well-known result (see also Ref. 6).

⁶For details, see D. Pines and J. R. Schrieffer, Phys. Rev. **124**, 1387 (1961).

⁷For details, see DuBois and Goldman (Ref. 1).

⁸N. Tzoar, Trans. IEEE **ED-17**, 245 (1970).

PHYSICAL REVIEW B

VOLUME 5, NUMBER 2

15 JANUARY 1972

Temperature Modulation of the Optical Constants of Layer Compounds GaSe and GaS

M. Grandolfo, F. Somma, and P. Vecchia

Physics Laboratory, Istituto Superiore di Sanità, Rome, Italy

(Received 15 June 1971)

We report the thermorefectance spectra of the layer compounds GaSe and GaS at liquid-nitrogen temperature in the energy interval 2–6 eV. The spectra were subjected to a Kramers-Kronig analysis, and the changes in the real and imaginary parts of the dielectric constant, induced by the temperature change of the samples, were obtained. The optical constants of the two materials were computed by processing the known reflectivity spectra. A phenomenological interpretation of the observed experimental results is presented. It is shown that under certain conditions it is necessary to invoke the presence of excitons at saddle-point singularities in order to achieve reasonable agreement between theory and experiment.

I. INTRODUCTION

Temperature modulation is observed as a change in the reflectance of a semiconductor induced by a periodic variation of the reflecting-surface temperature.^{1,2} Since the reflectance modulation gives rise to a pronounced structure of peaks at approximately the photon energies of interband transitions, this effect adds to the information on band-structure analysis extracted from optical studies on semiconductors. Moreover, the differential nature of the effect considerably enhances the structures in comparison with ordinary reflectance studies, providing much higher resolution and sensitivity.

Thermorefectance measurements on semiconductors and semimetals have been made by Batz on Ge,^{1,3} by Lange and Henrion on CdS and Se,⁴ by Balzarotti and Grandolfo on graphite⁵ and Si,⁶ by Matatagui, Thompson, and Cardona⁷ on seventeen semiconductors having diamond (Si), zinc-blende (AlSb, GaP, GaSb, InP, InAs, InSb, ZnS, ZnSe, ZnTe, CdTe, HgSe, and HgTe) and wurtzite (ZnO, CdS, and CdSe) structures, and more recently by Iliev and Assenov on CdS at the excitonic region⁸ and by Georgobiani and Fridrikh⁹ on ZnS near the fundamental absorption edge. All these experiments have demonstrated that the effect of a temperature variation on the optical properties of the material corresponds to a shift of the energy threshold and to a broadening of the involved critical points. The shift of the energy gap is caused by

two distinct mechanisms: the thermal expansion and the electron-phonon interaction. The broadening is only due to the electron-phonon interaction, and generally speaking this effect is small compared to the total shift. Experimental evidence, however, exists for a strong temperature modulation only of the broadening parameter at least in the case of M_1 saddle-point singularities in strongly anisotropic materials.⁵

In recent years the III-VI compound semiconductors such as GaSe and GaS have attracted considerable attention. Most of the studies have been concerned with the crystal structure,¹⁰ the electrical transport properties,¹¹ and the optical properties¹² in the vicinity of and well above the fundamental absorption edge. The crystal structures of GaSe and GaS are composed of isomorphous fourfold atomic layers and differ only in the way these layers are stacked. The Se and S atoms occupy equivalent sites, and the bonding between a multiple layer is predominantly covalent with a small ionic contribution. Owing to the fact that the bonding between layers is of the van der Waals type, the optical properties are largely governed by the structure of an individual fourfold layer; most of the theoretical work on the electronic structure of these compounds has therefore been based on a two-dimensional approximation, that is, the interaction between different crystal planes has not been taken into account.¹³

In this paper we present the results obtained by

thermally modulating the reflectivity of GaSe and GaS samples, at liquid-nitrogen temperature, and at near-normal incidence using unpolarized light, for photon energies up to about 6 eV. The energy dependence of the optical constants has been obtained by processing the known reflectivity spectra of GaSe and GaS. The experimental results have been thereby subjected to a Kramers-Kronig analysis in order to determine the phase changes $\Delta\theta$ and the corresponding changes in the real and imaginary parts of the dielectric constant of both materials. These derived spectra are then compared with theory in an attempt to identify the nature of the critical points giving rise to the transitions.

II. EXPERIMENTAL LAYOUT

The experimental arrangement that has been used is shown in Fig. 1. Light from a xenon lamp (Hanovia 976 C-1) was focused on the entrance slit of a Hilger and Watts D331 double-grating monochromator. The monochromatic light was focused on the samples, reflected at an angle of about 8° , and refocused on a Philips 56 TUVF photomultiplier. A resolution of 10 \AA or better was used, depending on the spectral region. The electronic system was the standard one in the technique of solid-state modulation spectroscopy. The dc portion of the output current from the photomultiplier, proportional to the reflectance of the sample R , is kept constant throughout the experiment by a servomech-

anism varying the photomultiplier power-supply voltage.¹⁴ The ac component, proportional to the reflectance change ΔR induced by the periodic temperature modulation, is detected by a Tekelec model No. TE 9000 lock-in amplifier, whose reference signal is supplied by the same square-wave generator that settles the modulation frequency and supplies power to heat the sample.

The advantage of using a square wave instead of a sine wave for thermal modulation is easily realized. If we define a modulation efficiency γ as the ratio of the modulation amplitude ΔT to the rise in the average temperature, it is possible to show² that in the two cases γ assumes the following expressions:

$$\gamma_{\text{square wave}} = \frac{4Q\tau}{\pi^2 C} = 0.405 \frac{Q\tau}{C}, \quad (1)$$

$$\gamma_{\text{sine wave}} = \frac{Q\tau}{\sqrt{2}\pi C} = 0.22 \frac{Q\tau}{C}, \quad (2)$$

where Q is the heat leak per unit time and unit temperature difference between samples and sapphire sink, τ is the period of the applied modulation voltage, and C is the heat capacity of the samples. By comparing Eq. (1) with Eq. (2) it is possible to realize that the efficiency γ is almost a factor of 2 higher for square-wave modulation than for sine waves. The frequency used was a compromise between signal strength and noise level and was usually fixed at 3 Hz. An x - y recorder si-

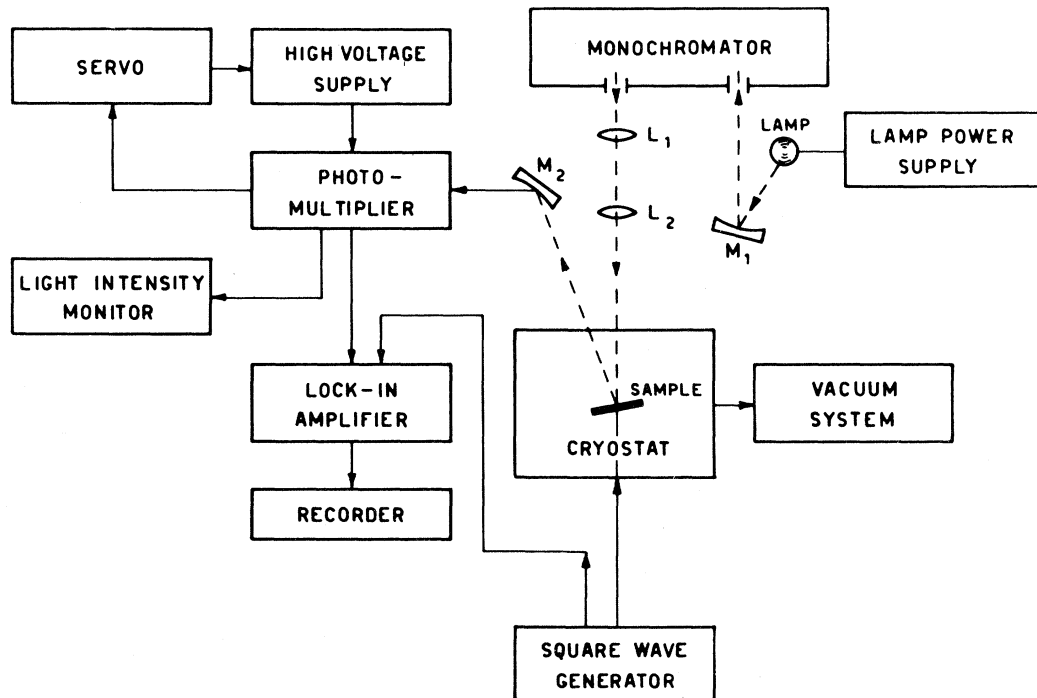


FIG. 1. Experimental setup for temperature-modulated reflectance measurements.

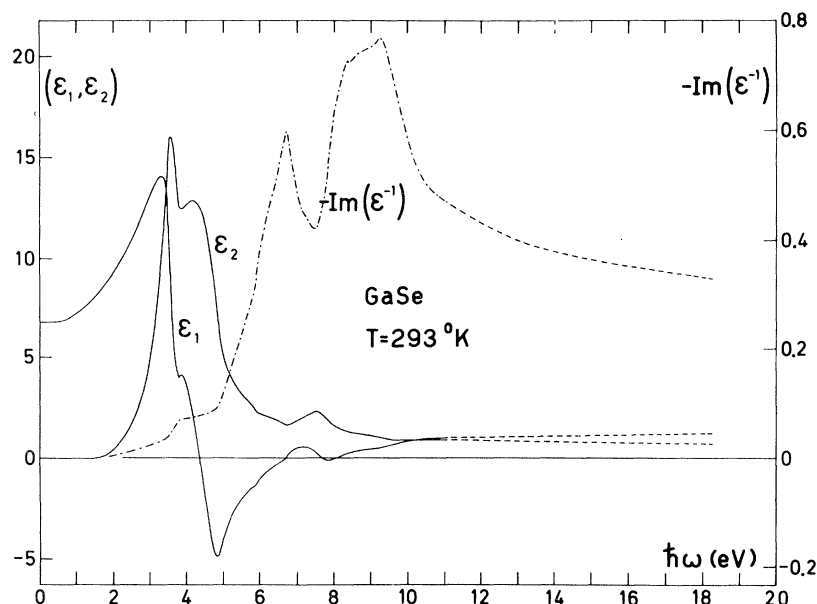


FIG. 2. Real and imaginary parts of the dielectric constant of GaSe (solid line) as obtained from the Kramers-Kronig transformation of the experimental spectrum R . The dot-dashed curve is the energy-loss function $-\text{Im} \epsilon^{-1}$ and the dashed line represents the extrapolated region.

multaneously receives at the y input the in-phase output of the amplifier and at the x input a voltage linearly varying with wavelength, so that the ratio $\Delta R/R$ versus wavelength is directly obtained. The crystals were in platelet form and the specimens suitable for reflectivity measurements were readily obtained by cleavage using a razor blade and not further treated. The samples were typically 10 mm long and 4 mm wide, with their thickness ranging from 50 to 300 μ . They were bonded with silicone grease to a vacuum-evaporated gold film on a sapphire substrate acting as a heat sink and mounted on the copper cold finger of a metal cryostat fitted with quartz windows. A vacuum of the order of 10^{-6} Torr was kept inside the cryostat while liquid nitrogen was added to the reservoir in order to measure at a fixed temperature. The dc temperature rise of the samples was measured by a thermocouple attached to their surfaces, away from the incoming light beam. The amplitude of the temperature modulation ΔT , although not accurately measured in our experiment, did not exceed 2 $^{\circ}\text{C}$.

III. RESULTS AND DISCUSSION

It was mentioned in Sec. I that the high spectral resolution allows one to observe a characteristic pattern in which the structure responds to the temperature changes. The extent to which this characteristic pattern can be evaluated in terms of type and location of critical points will depend upon a theoretical understanding and a subsequent analysis of the effect. The basis of such an analysis is provided by the relation between the periodic variation of temperature and the corresponding change

of the density-of-states function induced in the neighborhood of critical points by this variation. The measured values of $\Delta R/R$ are related to the variation $\Delta \epsilon_1$, $\Delta \epsilon_2$ of the real and imaginary parts of the complex dielectric constant by the well-known equation

$$\Delta R/R = \alpha(\epsilon_1, \epsilon_2)\Delta \epsilon_1 + \beta(\epsilon_1, \epsilon_2)\Delta \epsilon_2. \quad (3)$$

On the other hand, the quantities $\Delta \epsilon_1$ and $\Delta \epsilon_2$, whose physical meaning is more direct, may be deduced from the known values of $\Delta R/R$ by means

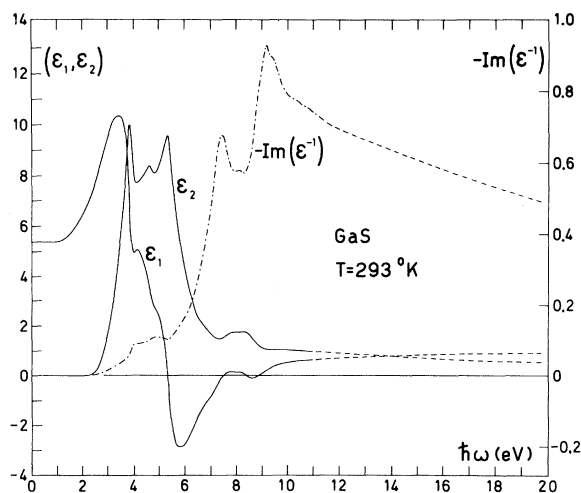


FIG. 3. Real and imaginary parts of the dielectric constants of GaS (solid line) as obtained from the Kramers-Kronig transformation of the experimental spectrum R . The dot-dashed curve is the energy-loss function $-\text{Im} \epsilon^{-1}$ and the dashed line represents the extrapolated region.

of the dispersion equations.

We obtained the values of ϵ_1 and ϵ_2 necessary for this computation by processing the absolute reflectivity spectra obtained by Bassani, Greenaway, and Fischer.¹⁵

We also obtained by the same calculation the real and imaginary parts n and k of the complex refractive index, the effective dielectric constant $\epsilon_{0,eff}$, the effective number of free electrons n_{eff} contributing to the optical properties, and the energy-loss function $-\text{Im}(1/\epsilon)$.

In Figs. 2 and 3 we show the spectral dependence of ϵ_1 , ϵ_2 , and $-\text{Im}(1/\epsilon)$ for GaSe and GaS, respectively, while the other above-mentioned quantities, not directly related to the experiment described in this paper, are reported elsewhere.¹⁶

It is evident that although the calculated optical constants are believed to be nearly correct at energies well below the limit of experimental data, more definitive results require a further extension of the reflectivity data into the ultraviolet region as well as a more refined extrapolation procedure.

The thermorefectance spectra at liquid-nitrogen temperature of GaSe and GaS are shown in Figs. 4 and 5, respectively. In the case of GaSe the dominant structure at about 2.09 eV arises from the direct-gap region and can be directly related to the temperature-modulated reflectance at the ground-state exciton line.¹⁷ At energies well above the fundamental edge, three structures at least are present.

The fractional reflectivity change of GaS presents only two prominent structures in the measured en-

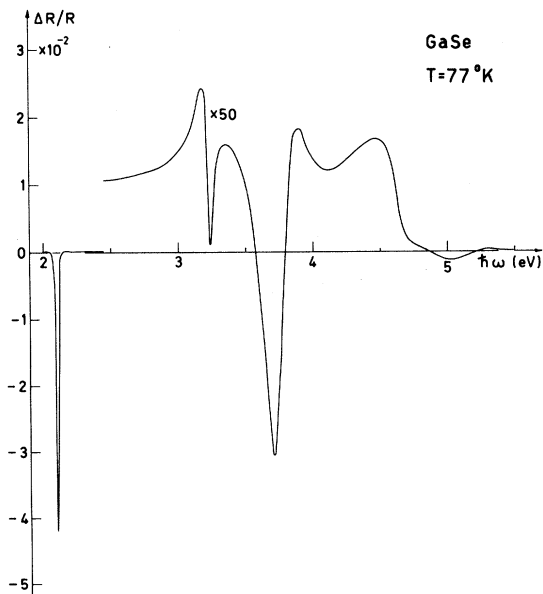


FIG. 4. Temperature-modulated reflectance spectrum of GaSe at 77 °K.

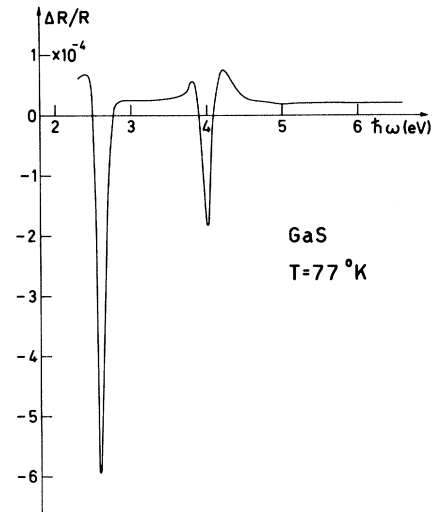


FIG. 5. Temperature-modulated reflectance spectrum of GaS at 77 °K.

ergy interval, corresponding to the fundamental edge region and to transitions at the point Q in the Brillouin zone.

One would be tempted to correlate directly the observed structures in the thermorefectance spectra with the band-structure critical points. In effect, the overlapping of the contributions of $\Delta\epsilon_1$

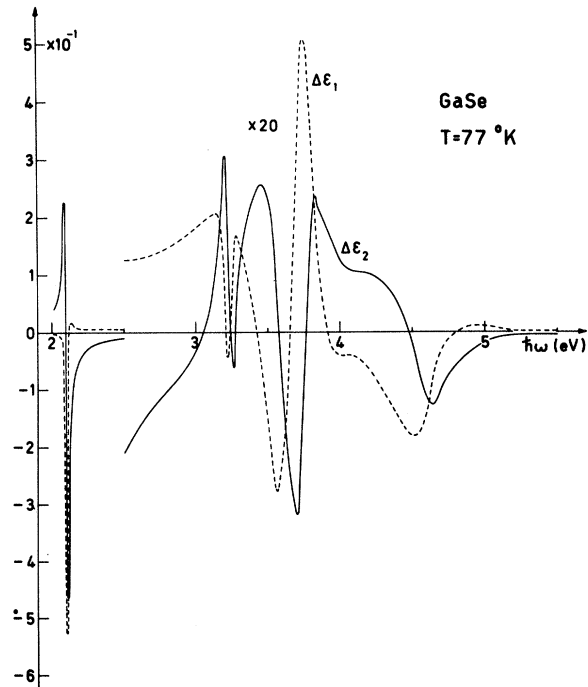


FIG. 6. $\Delta\epsilon_1$ (dashed line) and $\Delta\epsilon_2$ (solid line) for GaSe at liquid-nitrogen temperature as obtained from the Kramers-Kronig analysis of the data of Fig. 4.

and $\Delta\epsilon_2$ we reported above may generate accidental structures in $\Delta R/R$. Before proceeding to a discussion of the experimental results we will separate these terms by performing a Kramers-Kronig analysis of $\Delta R/R$ to extract from it $\Delta\epsilon_1$ and $\Delta\epsilon_2$.

By differentiation with respect to temperature of the dispersion relation

$$\frac{\Delta\vartheta(\omega)}{\Delta T} = \frac{1}{2\pi} \left[\left(\frac{1}{R} \frac{\Delta R}{\Delta T} \right)_{\omega=\omega_1} \ln \frac{\omega + \omega_1}{\omega - \omega_1} - 2\omega \int_{\omega_1}^{\omega - \Delta\omega} \frac{1}{R} \frac{\Delta R}{\Delta T} \frac{d\omega'}{\omega'^2 - \omega^2} + \left(\frac{1}{R} \frac{\Delta R}{\Delta T} \right)_{\omega=\omega_2} \ln \frac{2\omega - \Delta\omega}{2\omega + \Delta\omega} - 2\omega \int_{\omega + \Delta\omega}^{\omega_2} \frac{1}{R} \frac{\Delta R}{\Delta T} \frac{d\omega'}{\omega'^2 - \omega^2} \right], \quad (6)$$

where $\hbar\omega_1$ and $\hbar\omega_2$ are the limits of the experimental range. The value of $\hbar\Delta\omega$ used was chosen such that the error in $\Delta\vartheta/\Delta T$ was about 0.1%. The corresponding changes $\Delta\epsilon_1$ and $\Delta\epsilon_2$ can be evaluated from the experimental values of $(1/R)\Delta R/\Delta T$ and the calculated values of $\Delta\vartheta/\Delta T$ taking into account the expressions relating the optical constants ϵ_1 , ϵ_2 , r , and ϑ . One obtains

$$\Delta\epsilon_1 = A(\epsilon_1, \epsilon_2) (\Delta R/R) + B(\epsilon_1, \epsilon_2) \Delta\vartheta, \quad (7a)$$

$$\Delta\epsilon_2 = -\frac{1}{2} B(\epsilon_1, \epsilon_2) (\Delta R/R) + 2A(\epsilon_1, \epsilon_2) \Delta\vartheta. \quad (7b)$$

This computation was carried out for all the experimental data, using the computed values of ϵ_1 and ϵ_2 to deduce the coefficients A and B . The results for the cases of Figs. 4 and 5 are shown in Figs. 6 and 7, respectively.

In order to achieve a phenomenological interpretation of the observed experimental results we focus our attention initially on the strong dispersionlike shape of $\Delta\epsilon_2$ appearing in correspondence with the strong negative peaks in the thermorefectance spectra of the two materials in the vicinity of the gap region. The exciton-phonon interaction practically determines the line shape of the excitonic structures, and leads to a Lorentzian shape of the line, at least for the ground-state exciton line. The temperature effect can be accounted for by two distinct mechanisms: a shift ΔE of the line without broadening, or a symmetrical broadening $\Delta\Gamma$ without shift. In the former case, differentiation of ϵ_2 with respect to $E = \hbar\omega$ gives the following result:

$$\Delta\epsilon_2 = \frac{(\hbar\omega - E_c + \frac{1}{2}\Delta E)\Gamma}{[(\hbar\omega - E_c + \Delta E)^2 + \frac{1}{4}\Gamma^2][(\hbar\omega - E_c)^2 + \frac{1}{4}\Gamma^2]} \Delta E, \quad (8)$$

while in the latter one we get

$$\Delta\epsilon_2 = \frac{(\hbar\omega - E_c)^2 - \frac{1}{4}\Gamma^2 - \frac{1}{2}\Gamma\Delta\Gamma}{[(\hbar\omega - E_c)^2 + (\frac{1}{2}\Gamma + \Delta\Gamma)^2][(\hbar\omega - E_c + \frac{1}{4}\Gamma^2)]} \Delta\Gamma, \quad (9)$$

where E_c is the energy position of the structure, Γ

$$\vartheta(\omega) = \frac{2\omega}{\pi} \wp \int_0^\infty \frac{\ln r(\omega')}{\omega'^2 - \omega^2} d\omega', \quad (4)$$

we obtain

$$\frac{\Delta\vartheta(\omega)}{\Delta T} = \frac{2\omega}{\pi} \wp \int_0^\infty \frac{1}{R} \frac{\Delta R}{\Delta T} \frac{d\omega'}{\omega'^2 - \omega^2}. \quad (5)$$

This integral can be transformed¹⁸ into

is the Lorentzian parameter, and ΔE and $\Delta\Gamma$ are their temperature modulations. An attempt has been made to fit the experimental $\Delta\epsilon_2$ line shapes with expression (8) or (9) or a linear combination of both. The fitting was made by the least-squares method, and the best fit was found using expression (8). The experimental behavior of the ground-state exciton lines seems to be accounted for (Figs. 8 and 9) in terms of only a nearly rigid shift of the whole structure to lower energies. The agreement with the experiment is rather good taking $E_0 = 2.093$ eV and $\Gamma = 41.0$ meV for GaSe, and $E_0 = 2.646$ eV and $\Gamma = 187.5$ meV for GaS. From the

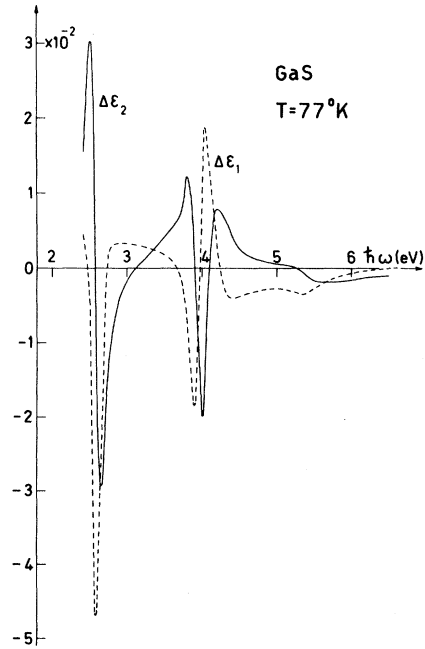


FIG. 7. $\Delta\epsilon_1$ (dashed line) and $\Delta\epsilon_2$ (solid line) for GaS at liquid-nitrogen temperature as obtained from the Kramers-Kronig analysis of the data of Fig. 5.

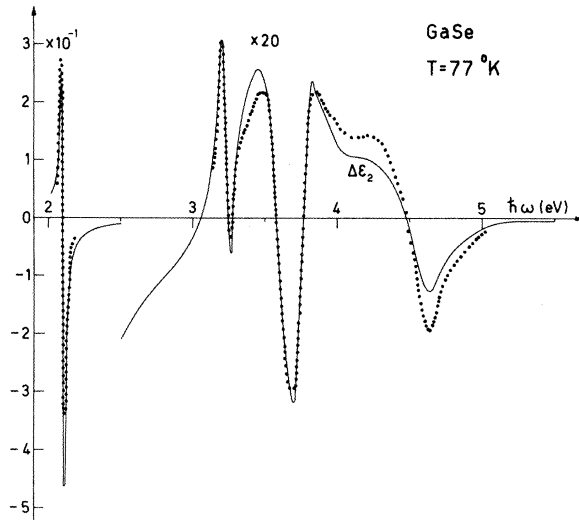


FIG. 8. Comparison between the experimental temperature-induced change in ϵ_2 for GaSe at liquid-nitrogen temperature (solid line) and the change calculated (black points) from the overlapping contributions of the structures arising from the energy-gap region and the saddle-point singularities. The M_1 critical point located at 3.658 eV has been interpreted taking into account exciton effects.

computed values of ΔE we estimate a temperature modulation ΔT of about 2°K . The temperature dependence of the exciton lines has also been measured and temperature coefficients of -5.49×10^{-4} and -7.20×10^{-4} eV/ $^\circ\text{K}$ have been found for GaSe and GaS, respectively, in fairly good agreement with the values obtained by other authors.¹⁹

At energies well above the gap both compounds present strong structures which can be conveniently related to the energy-band-scheme calculations of Bassani and Parravicini²⁰ and Kamimura and Nakao.²¹ These authors derived the detailed structures of the conduction and valence bands of GaSe and GaS, pointing out the existence of two-dimensional pair bands corresponding to transitions between π bands. From the evaluated band structures strong peaks appear in the joint density of states of the two materials, in correspondence with transitions at the Q point of the Brillouin zone, owing to the fact that in this band scheme Q is a saddle point. These peaks remain in $\epsilon_2(0, \omega)$ and correspond to the peaks obtained from absolute-reflectivity experiments both in GaSe and GaS. They give rise in the thermorefectance spectra to the structures located at about 3.6 and 3.9 eV in GaSe and GaS, respectively. It is well known that in the two-dimensional approximation, which consists of neglecting the interaction between different layer planes, the critical points reduce to those of M_0 and M_1 type, giving rise, respectively, to step and logarithmic singularities in the joint density of

states. Experimental results previously obtained by thermally modulating the optical constants of another layer-type compound such as graphite⁵ suggested that for this material the effect of temperature is mainly to shift the M_0 critical point and to broaden the M_1 saddle-point singularity occurring at Q in the Brillouin zone. An attempt has then been made to fit the line shapes of $\Delta\epsilon_2$ in the vicinity of 3.6 and 3.9 eV in GaSe and GaS with Eq. (9), representing, as in the case of graphite, a symmetrical broadening without a shift of the Lorentzian line describing the M_1 logarithmic singularity. As in the case of GaS, recently reported,²² the result of the fit of Eq. (9) for GaSe is so poor also that we are led to recognize the failure of the one-electron model in correctly interpreting the observed line shape. Figures 8 and 9 show a comparison of our experimental results with the theoretical behavior resulting from application of Toyozawa's theory.²³ The black dots are obtained assuming that the observed structures arise from a unique critical point built up from the metamorphism of the two possible van Hove singularities (M_1 and M_0), taking into account that the effect of temperature, as observed in the case of graphite, is to shift one of the critical points (M_0) and to broaden the other one (M_1) because of the electron-phonon interaction. The lifetime broadening of the M_0 point has been introduced through a convolution integral, using a Lorentzian parameter Γ . The only adjustable parameters were the energy position E_1 and the lifetime-broadening pa-

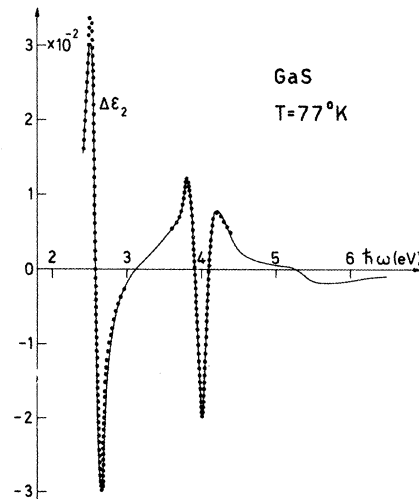


FIG. 9. Comparison between the experimental temperature-induced change in ϵ_2 for GaS at liquid-nitrogen temperature (solid line) and the change calculated (black points) from the overlapping contributions of the structures arising from the energy-gap region and the saddle-point singularities. The M_1 critical point located at 3.998 eV has been interpreted taking into account exciton effects.

parameter Γ . The calculated results, obtained by mixing the line shapes expected for M_1 and M_0 critical points and taking into account the different effects of the modulating perturbation, give $E_1 = 3.658 \pm 0.001$ eV and $\Gamma = 0.256 \pm 0.001$ eV for GaSe, and $E_1 = 3.993 \pm 0.001$ eV and $\Gamma = 0.289 \pm 0.001$ eV for GaS. We feel that the good agreement between the experimental curves and the points calculated on the basis of the metamorphism of critical points provides strong evidence that the exciton model describes quite well, also in a two-dimensional crystal, the effect of the Coulomb interaction upon the direct interband transitions above the fundamental edge.

The additional structure clearly seen in GaSe at 3.255 eV can be tentatively assigned to transitions at some point in the q direction and related to the shoulder present at the low-energy side of the E_1 peak in the absolute-reflectivity measurements. In Fig. 8 we show the results obtained by fitting this structure with a s -shaped line partially superimposed on the structure centered at $E_1 = 3.658$ eV. The best fit is obtained by positioning the singularity at 3.255 eV with a Lorentzian parameter $\Gamma = 0.022$ eV. The effect of the temperature at this singularity seems to be a shift of the structure to lower energies rather than a simple lifetime broad-

ening as for the saddle-point singularity at 3.658 eV.

Finally, a few words should be said about the presence at the high-energy side of the spectra of additional structures, more pronounced in GaSe than in GaS.

From the preceding analysis of the line shapes we were able to deduce that, with the exception of the singularities strongly affected by the residual Coulomb interaction, the temperature derivative of the optical constants behaves to some extent as their frequency derivative. Accordingly, we are led to locate the main singularities at the zeros of the $\Delta\epsilon_2$ curve. From this point of view we locate these structures at 4.577 and 5.260 eV for GaSe and GaS, respectively.

ACKNOWLEDGMENTS

The authors are much indebted to Dr. A. Balzarotti and Dr. E. Tabet for a number of profitable discussions and valuable suggestions. Thanks are due to G. Mariutti and C. Ramoni for the preparation of the samples and to R. Crateri, G. Di Nunzio, and R. Felici for their valuable technological assistance. We are also very grateful to P. Corradini and A. Verdecchia for the solution of many computing problems.

¹B. Batz, *Solid State Commun.* **4**, 241 (1966).

²M. Cardona, *Modulation Spectroscopy* (Academic, New York, 1969).

³B. Batz, *Solid State Commun.* **5**, 985 (1967).

⁴H. Lange and W. Henrion, *Phys. Status Solidi* **23**, K67 (1967).

⁵A. Balzarotti and M. Grandolfo, *Phys. Rev. Letters* **20**, 9 (1968).

⁶A. Balzarotti and M. Grandolfo, *Solid State Commun.* **6**, 815 (1968).

⁷E. Matatagui, A. G. Thompson, and M. Cardona, *Phys. Rev.* **176**, 950 (1968).

⁸M. Iliev and I. Assenov, *Phys. Status Solidi* **42**, 383 (1970).

⁹A. N. Georgobiani and Kh. Fridrikh, *Fiz. Tverd. Tela* **12**, 1086 (1970) [*Sov. Phys. Solid State* **12**, 849 (1970)].

¹⁰Z. S. Basinsky, D. B. Dove, and E. Mooser, *Helv. Phys. Acta* **34**, 373 (1961).

¹¹P. Fielding, G. Fischer, and E. Mooser, *J. Phys. Chem. Solids* **8**, 434 (1959); R. Fivaz and E. Mooser, *Phys. Rev.* **163**, 743 (1967).

¹²J. L. Brebner and G. Fischer, *Proceedings of the International Conference on the Physics of Semiconductors, Exeter*, 1962 (Institute of Physics and the Physical Society, London, 1962); J. L. Brebner, *J. Phys. Chem. Solids* **25**, 1427 (1964); N. A. Gasanova and G. Akhundov, *Opt. i Spektroskopiya* **20**, 193 (1966) [*Sov. Phys. Opt. Spectry.* **20**, 193 (1966)].

¹³L. Van Hove, *Phys. Rev.* **89**, 1189 (1953); G. F. Bassani, in *Proceedings of the International School of Physics, Varenna, Course XXXIV*, edited by J. Tauc (Academic, New York, 1966).

¹⁴C. Felici and C. Ranghiasi, Istituto Superiore di Sanità Physical Labs, Report No. ISS 71/9, 1971 (unpublished).

¹⁵F. Bassani, D. L. Greenaway, and G. Fischer, in *Proceedings of the Seventh International Conference on the Physics of Semiconductors, Paris*, 1964 (Academic, New York, 1965).

¹⁶M. Grandolfo, F. Somma, and P. Vecchia, Istituto Superiore di Sanità Physical Labs, Report No. ISS 71/9, 1971 (unpublished).

¹⁷A. Balzarotti, M. Grandolfo, F. Somma, and P. Vecchia, *Phys. Status Solidi* **44**, 713 (1971).

¹⁸A. Frova, P. J. Boddy, and Y. S. Chen, *Phys. Rev.* **157**, 700 (1967).

¹⁹Y. Suzuki, Y. Hamakawa, H. Kimura, M. Komiya, and S. Ibuki, *J. Phys. Chem. Solids* **31**, 2217 (1970).

²⁰F. Bassani and G. Pastori Parravicini, *Nuovo Cimento* **50B**, 95 (1967).

²¹H. Kamimura and K. Nakao, *J. Phys. Soc. Japan* **24**, 1313 (1968).

²²M. Grandolfo, F. Somma, and P. Vecchia, *Phys. Rev. B* **3**, 3485 (1971).

²³B. Velicky and J. Sak, *Phys. Status Solidi* **16**, 147 (1966); Y. Toyozawa, H. Inoue, T. Inui, M. Okazaki, and E. Hanamura, *J. Phys. Soc. Japan* **22**, 1337 (1967).